Earth, Planets and Space
a SpringerOpen Journal

FULL PAPER Open Access

How does ionospheric TEC vary if solar EUV irradiance continuously decreases?

Yiding Chen[1,2*], Libo Liu[1,2], Huijun Le[1,2] and Weixing Wan[1,2]

Abstract

It is an interesting topic how the ionosphere varies when solar extreme ultraviolet (EUV) irradiance decreases far below normal levels. When extrapolating the total electron content (TEC)-EUV relation, significantly negative TECs at the zero solar EUV point are obtained, which indicates that TEC-EUV variation under extremely low solar EUV (ELSE) conditions does not follow the TEC-EUV trend during normal solar cycles. We suggest that there are four types of nonlinear TEC-EUV variations over the whole EUV range from zero to the solar maximum level. The features of the ionosphere under ELSE conditions were investigated using the TEC extrapolated with cubic TEC-EUV fitting. With the constraint of zero TEC at zero EUV, the cubic fitting takes not only observations but also the trend of the ionosphere (only an extremely weak ionosphere can exist when EUV vanishes) into account. The climatology features of TEC under ELSE conditions may differ from those during normal solar cycles at nighttime. Ionospheric dynamic processes are supposed to still significantly affect the ionosphere under ELSE conditions and induce this difference. With solar EUV decreasing, global electron content (GEC) should vary largely in accordance with the GEC-EUV trend during normal solar cycles, and the seasonal fluctuation of GEC declines, owing to the contraction of the ionosphere.

Keywords: Ionosphere; Total electron content; Nonlinear variation

Background

Variations of solar extreme ultraviolet (EUV) irradiance are important for the ionosphere and thermosphere. The prominent 11-year solar cycle variation of EUV has been widely investigated; meanwhile, variations of EUV over longer timescales have also drawn wide attention. Solar EUV is well correlated with the sunspot number, an important solar activity proxy, during normal solar cycles; specifically, EUV decreases as the sunspot number declines. Based on the sunspot historical record, Eddy (1976) justified the existence of an extremely low solar activity period known as the Maunder Minimum (1645 to 1715 A.D.) during which virtually no sunspots were observed. It is unclear how solar EUV and also the ionosphere varied during the extended extremely low solar activity periods such as the Maunder Minimum. Some researchers have attempted to derive the EUV irradiance during these extreme periods by solar irradiance models (e.g., Lean et al. 2011); the results reveal that EUV irradiance potentially decreased to an extremely low level during the Maunder Minimum period (see Figure 1).

Solar activity has recently undergone a deep minimum during 2007 to 2009. This solar minimum lasted longer than several previous minima, and the sunspot record during this solar minimum reached the lowest level after 1913. Solar EUV irradiance was found to have significantly decreased during this deep solar minimum (Didkovsky et al. 2010), and accordingly, the thermospheric density and ionospheric electron density declined (e.g., Chen et al. 2011; Emmert et al. 2010; Liu et al. 2011; Solomon et al. 2010). The 2007 to 2009 deep solar minimum merely offered us a glimpse for understanding the Sun and the space environment during extremely low solar activity periods. As far as extremely deep solar minima, such as the Maunder Minimum, are concerned, solar EUV could potentially decrease to very low levels during these periods. Then, an important question remains about what is the possible state of the ionosphere under this extreme solar activity condition. Although no observation can directly provide us an answer, this topic is interesting and essential as another extremely low solar activity period could possibly come in the future.

* Correspondence: chenyd@mail.iggcas.ac.cn
[1]Key Laboratory of Ionospheric Environment, Institute of Geology and Geophysics, Chinese Academy of Sciences, Beijing 100029, China
[2]Beijing National Observatory of Space Environment, Institute of Geology and Geophysics, Chinese Academy of Sciences, Beijing 100029, China

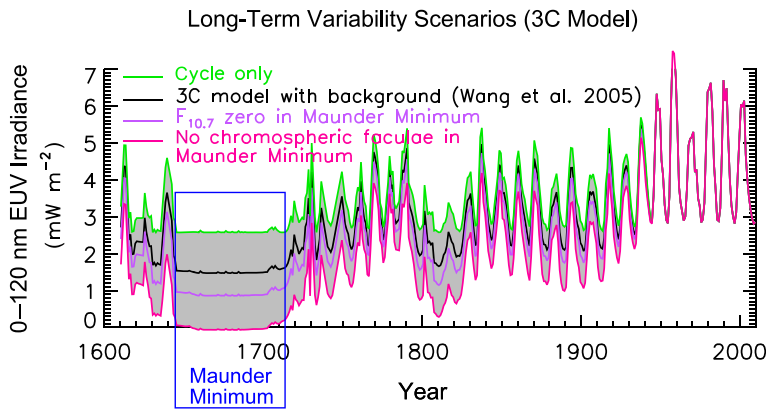

Figure 1 Annually averaged solar EUV irradiance (0 to 120 nm) estimated with solar EUV models. Solar EUV irradiance potentially decreased to an extremely low level during the Maunder Minimum period (after Lean et al. 2011).

A few studies have investigated the state of the ionosphere under the conditions of extremely low solar EUV (ELSE), which means solar EUV irradiance is much lower than the normal solar minimum level. Liu et al. (2009) revealed that ionospheric total electron content (TEC) is negative at the zero EUV point if it decreases with EUV in accordance with the linear TEC-EUV relation during recent lower solar activity periods. The negative TEC is nonphysical and thus indicates that ionospheric variation with EUV under ELSE conditions should be different from that during recent lower solar activity periods. Smithtro and Sojka (2005) simulated the behavior of the ionosphere under extremely low solar flux conditions using a global average ionosphere and thermosphere model. Their results showed that as solar irradiance falls below normal solar minimum levels, the concentration of O^+ decreases rapidly relative to the molecular ions so that the ratio of f_oF_2/f_oF_1 approaches unity (f_oF_1 and f_oF_2 are the critical frequencies of the F_1 and F_2 layers, respectively), which indicates that the vertical profile of the ionosphere may significantly change under extremely low solar flux conditions. The abovementioned studies indicate that to some extent, the behavior of the ionosphere under ELSE conditions is possibly different from that under normal solar cycle conditions.

This paper deals with the behavior of TEC under ELSE conditions using the Jet Propulsion Laboratory (JPL) TEC maps (Iijima et al. 1999; Mannucci et al. 1998) and the solar EUV data observed by the Solar EUV Monitor aboard the Solar Heliospheric Observatory satellite (SOHO/SEM) (Judge et al. 1998). We discuss the nonlinear variation trend of TEC with EUV and some primary climatology features of TEC under ELSE conditions. The results highlight the nonlinear variations of TEC with EUV and some climatology features of TEC under ELSE conditions that are different from those during the normal solar cycle period.

Methods

Data used

Daily EUV flux monitored by SOHO/SEM has been continuously provided since 1996. It is an ideal dataset for investigating EUV's longer-term variations, such as the solar cycle variation, and their effects on the ionosphere. In this study, SOHO/SEM EUV integral flux over 0.1- to 50-nm wavelength range was used to present the variations of the EUV irradiance that causes the ionization of neutral atmosphere.

As Smithtro and Sojka (2005) revealed, the vertical profile of the ionosphere during ELSE periods is possibly significantly different from that during normal solar cycles. Thus, some characteristic parameters corresponding to the key layers of the ionosphere (e.g., peak electron density of the F_2 layer) are possibly inapplicable under ELSE conditions. TEC is a parameter that depends on the altitudinal integral of the electron density; it always can be used to detect the state of the ionosphere if only the ionosphere exists. In this paper, we discuss ionospheric behavior under ELSE conditions based on the parameter TEC. The JPL TEC maps have been routinely released since 1998; they are essential for investigating the global features and solar activity variations of the ionosphere. The JPL TEC maps are analytic descriptions of the measured slant TEC; the accuracy of the maps depends on the numbers of global positioning system (GPS) receiver stations and satellites available. There are several other TEC map datasets such as ESA, UPC, and CODE (Hernández-Parajes et al. 2009). Some differences still exist between these different TEC datasets. We used the JPL TEC maps in this study. The TEC values at given local times were obtained by interpolating JPL TEC to local time grids. In order to suppress the effect of stronger geomagnetic disturbance, the TEC data were removed in the analyses if the *Ap* index in the current day of TEC or in the previous day of TEC is larger than 30.

Does ELSE TEC follow the TEC-EUV relation during normal solar cycles?

During normal solar cycles, the variation of ionospheric electron density with solar EUV flux is nearly linear at lower solar activities and nonlinear at higher solar activities. At higher solar activity levels, the electron density varies with solar EUV flux in a pattern that deviates from the linear trend at lower solar activities (e.g., Balan et al. 1994; Chen and Liu 2010; Liu et al. 2006; Richards 2001). Some studies revealed that quadratic regression fits could be used to well estimate the nonlinear variation of the electron density with EUV flux during normal solar cycles (e.g., Chen et al. 2008; Gupta and Singh 2001; Sethi et al. 2002). If solar EUV continuously decreases to ELSE levels, does the electron density variation follow the linear or nonlinear relation between the electron density and EUV flux during normal solar cycles?

Solar EUV irradiance causes the vast majority of the ionization in the middle- and low-latitude ionosphere. If solar EUV irradiance vanishes, it can be deduced that only an extremely weak ionosphere can exist, owing to the weak ionization caused by the minor ionization sources such as starlight (e.g., Titheridge 2000). TEC should approach extremely low values, as compared with the TEC values during normal solar cycles, if solar EUV continuously decreases so that it approaches zero. Hence, we may investigate whether TEC under ELSE conditions varies with EUV irradiance following the linear or nonlinear TEC-EUV relation during normal solar cycles by extrapolating the linear or nonlinear TEC-EUV relation to the zero EUV point.

Figure 2 shows the variation of noontime TEC over a specific location (90°W, 40°S) with 0.1- to 50-nm EUV flux during the December to January season. The solid line in Figure 2a demonstrates the linear TEC-EUV regression fitting. The linear fitting was only for the data over the lower EUV range (here, EUV < 4×10^{14} photons/m^2/s) as the linear TEC-EUV variation is generally only valid for lower solar activity levels, whereas nonlinearity becomes important at higher solar activity levels. The TEC value at the zero EUV point was obtained by extrapolating the linear TEC-EUV fitting to the zero EUV point, as shown by the dashed line in Figure 2a. According to the method shown in Figure 2a, the TEC values at the zero EUV point were derived for different locations and seasons, and the data are shown in the left panels of Figure 3. In general, negative TEC values are dominant when EUV sufficiently approaches zero. The negative TEC is nonphysical; this indicates that TEC-EUV variation should differ from the linear TEC-EUV variation at lower solar activities (i.e., nonlinear variation) when solar EUV continuously decreases to extremely low levels. Then, we addressed the question of whether the nonlinear TEC-EUV relation during normal solar cycles

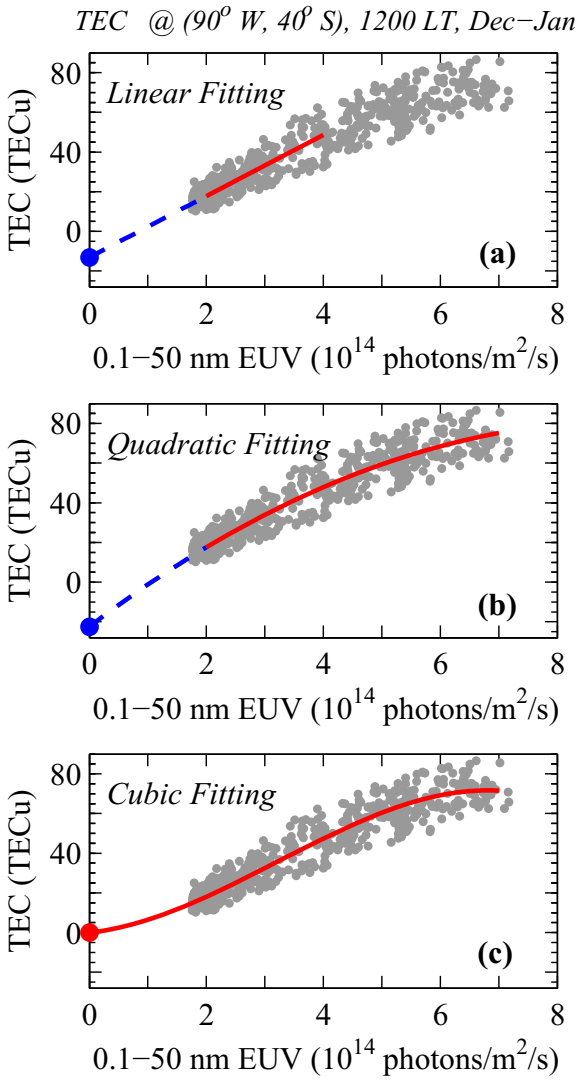

Figure 2 The demonstrations of total electron content (TEC)-EUV regression fitting. Linear fitting for the data of EUV < 4 **(a)**, quadratic fitting for the data of the full EUV range **(b)**, and cubic fitting for the data of the full EUV range and constrained with the term of zero TEC at zero EUV **(c)**.

can describe the nonlinear TEC-EUV variation under ELSE conditions. In Figure 2b, the solid line shows the quadratic TEC-EUV regression fitting for the observed data during normal solar cycles, and the dashed line demonstrates how the TEC value at the zero EUV point was obtained by extrapolating the quadratic fitting to the zero EUV point. According to the method shown in Figure 2b, TEC values at the zero EUV point were derived for different locations and seasons again, and the data are shown in the right panels of Figure 3. The quadratic extrapolated TEC is also significantly negative at low latitudes, which indicates that the quadratic TEC-EUV trend during normal solar cycles

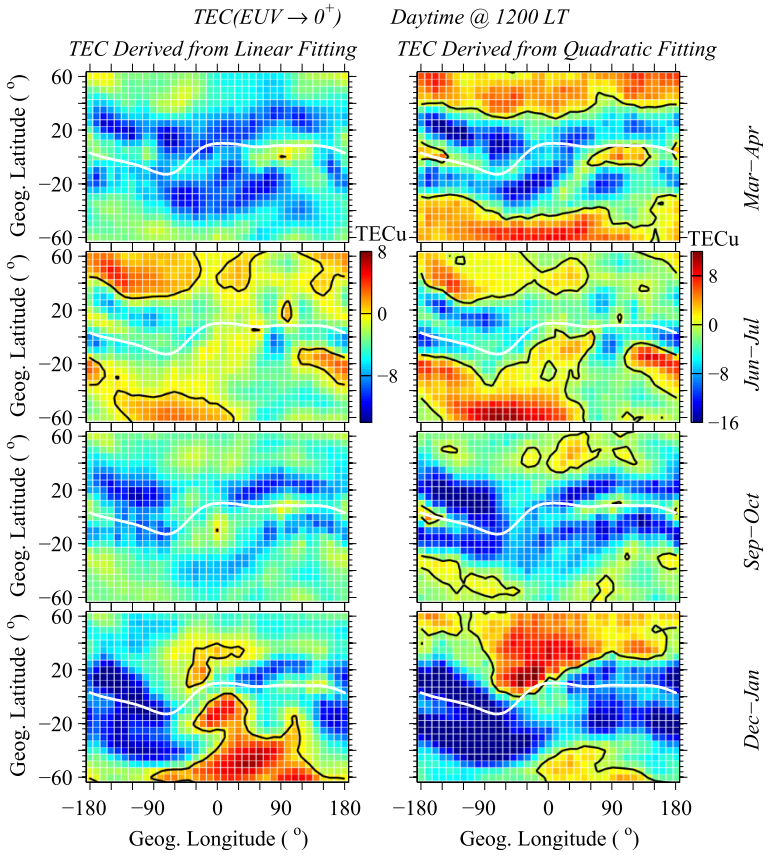

Figure 3 The TEC values at the zero solar EUV point. The left column is the TEC extrapolated from the linear TEC-EUV fitting for which the data of EUV < 4 were used (see Figure 2a), and the right column is the TEC extrapolated from the quadratic TEC-EUV fitting for which the data of the full EUV range were used (see Figure 2b). The white lines denote the dip equator, and the black contours denote zero TEC.

also cannot describe the TEC-EUV variation under ELSE conditions.

Method of extrapolating ELSE TEC

Both the TEC-EUV variations during normal solar cycles and under ELSE conditions are nonlinear, and the quadratic TEC-EUV relation during normal solar cycles cannot describe the TEC-EUV variation under ELSE conditions. This indicates that higher-order (cubic) TEC-EUV fitting is potentially needed to fully describe the TEC-EUV variation over the whole EUV range from zero to the solar maximum level. The minor ionization sources such as starlight, whose strength is lower than solar EUV strength during normal solar cycles by up to a factor of four (e.g., Strobel et al. 1974; Titheridge 2000), only can maintain an extremely weak ionosphere if solar EUV irradiance vanishes. This extremely weak ionosphere should be the limit of the normal ionosphere under the condition that solar EUV closely approaches zero, and its TEC value should be lower than the normal TEC value by up to a factor of four if simply estimating from the irradiance strength. For simplicity, this very minor TEC at the zero solar EUV point may be ignored when fitting TEC-EUV relationships as we do not discuss the ionosphere under the condition that EUV sufficiently approaches zero. In this paper, the TEC values under the ELSE conditions were obtained by extrapolating cubic TEC-EUV fitting to ELSE conditions. The cubic fitting was constrained with the term of zero TEC at zero EUV. The solid line in Figure 2c demonstrates the cubic TEC-EUV regression fitting.

Since both the TEC-EUV variations over the two EUV segments, from zero to the solar minimum level and from the solar minimum level to the solar maximum level, are nonlinear, the nonlinearities over the two EUV segments may have identical or contrary trends (for example, a TEC-EUV increase rate that increases with increasing EUV values would be indicative of an amplification trend, whereas a TEC-EUV increase rate that decreases with increasing EUV values would be indicative of a saturation trend). Over the whole EUV range from zero to the solar maximum level, the variation of TEC with EUV generally can be presented by four types of nonlinear trends. Figure 4 shows the sketches (the left panels) and the typical observation examples (the right panels) of the

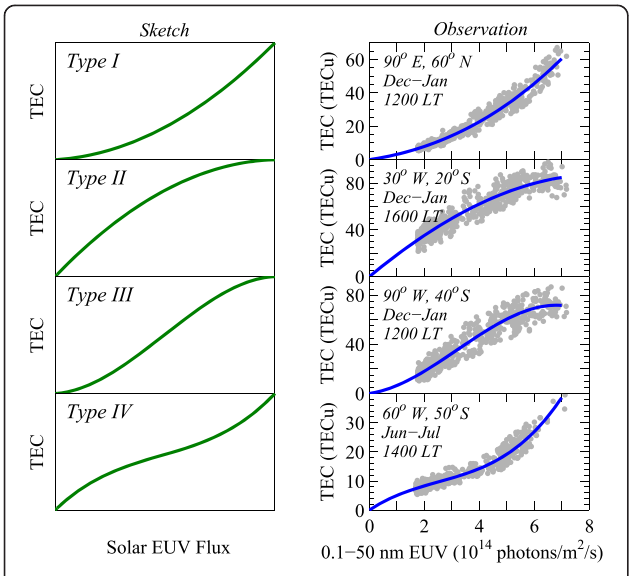

Figure 4 Sketches of four types of nonlinear TEC-EUV variations (left) and the corresponding observed examples (right). The solid lines in the right panels are the cubic fittings constrained with the term of zero TEC at zero EUV.

four types of nonlinear trends. Types I and II correspond to identical nonlinear trends over the two segments, while types III and IV correspond to contrary nonlinear trends over the two segments. The cubic TEC-EUV fitting can be used to well describe these nonlinear TEC-EUV variations.

Results and discussion

Some climatology features of the extrapolated TEC were investigated and compared with the features during the normal solar cycle period. We took the solar EUV level of 0.1- to 50-nm EUV flux equal to 1×10^{14} photons/m^2/s (nearly half of the 2007 to 2009 solar minimum level) as the typical ELSE condition, and for the normal solar cycle condition, we took the solar EUV level of 0.1- to 50-nm EUV flux equal to 3×10^{14} photons/m^2/s (a lower solar activity level) as a representative.

The equatorial ionization anomaly (EIA) induced by the equatorial fountain effect is a well-known latitudinal structure of the daytime ionosphere (e.g., Appleton 1946; Hanson and Moffett 1966). The EIA structure is characterized by a plasma density trough around the dip equator sandwiched by two off-equator peaks of the plasma density in the F_2 peak region, and it also appears in TEC's latitudinal distribution. Figure 5 shows the longitudinal and latitudinal distributions of noontime TEC under the normal solar cycle (the left panels) and ELSE (the right panels) conditions. The EIA structure is distinct and seasonally dependent under the normal solar cycle condition, and the extrapolated TEC shows that the EIA structure still exists under the ELSE condition. This indicates that the equatorial fountain effect still significantly controls the low-latitude ionosphere even when solar EUV decreases to a very low level. Fejer et al. (1991, 2008) revealed that the dependence of daytime equatorial vertical plasma drift, which drives the fountain effect, on solar irradiance flux is not prominent during the normal solar activity period. If that is still the case under ELSE conditions, equatorial vertical plasma drift is potentially efficient enough to induce the EIA structure.

Figure 6 shows the longitudinal and latitudinal distributions of nighttime TEC under the normal solar cycle (the left panels) and ELSE (the right panels) conditions. Under the normal solar cycle condition, TEC peaks at the dip equator during equinoxes and at a low-latitude band of the summer hemisphere during solstices. At nighttime, with the vanishing of the equatorial fountain effect, the EIA structure disappears except at solar maxima when the pre-reversal enhancement of the upward plasma drift induces a strong EIA at sunset, which can last to nighttime (e.g., Chen et al. 2009). There is no EIA structure after sunset at lower solar activity levels as the pre-reversal enhancement of the upward plasma drift is positively correlated with the solar activity level (e.g., Fejer et al. 1991). Under the ELSE condition, the extrapolated TEC shows different latitudinal variations from those under the normal solar cycle condition. An important feature is that TEC is higher at the mid-latitude bands where dips are close to ±45°.

Photoionization basically disappears at middle and low latitudes during the nighttime. The state of the nighttime ionosphere is related to recombination loss, the state of the daytime ionosphere, and ionospheric dynamics factors including neutral winds. Under ELSE conditions, the latitudinal structure of nighttime TEC is possibly related to the effect of neutral winds. The weakening and the subsequent reversal of daytime poleward wind, which takes place around sunset, may uplift the ionosphere to higher altitudes so that recombination loss slows down according to the servo theory (Rishbeth et al. 1978), and the efficiency of the meridional wind peaks at the latitude where dip equals ±45° (e.g., Rishbeth 1972). Moreover, neutral winds were revealed to increase with decreases in solar activity, owing to the decrement of ion drag induced by the decline of ion density when solar activity decreases (Kawamura et al. 2000; Liu et al. 2004). Thus, under ELSE conditions, the effect of neutral winds possibly plays an important role in the latitudinal distribution of nighttime TEC.

The effect of neutral winds may be detected by investigating local time variations of TEC. Figure 7 shows local time variations of the cubic fitted TEC under the normal solar cycle (the top panels) and ELSE (the bottom panels) conditions. Under the ELSE condition, the bottom panels of Figure 7 indicate that the attenuation of TEC since the

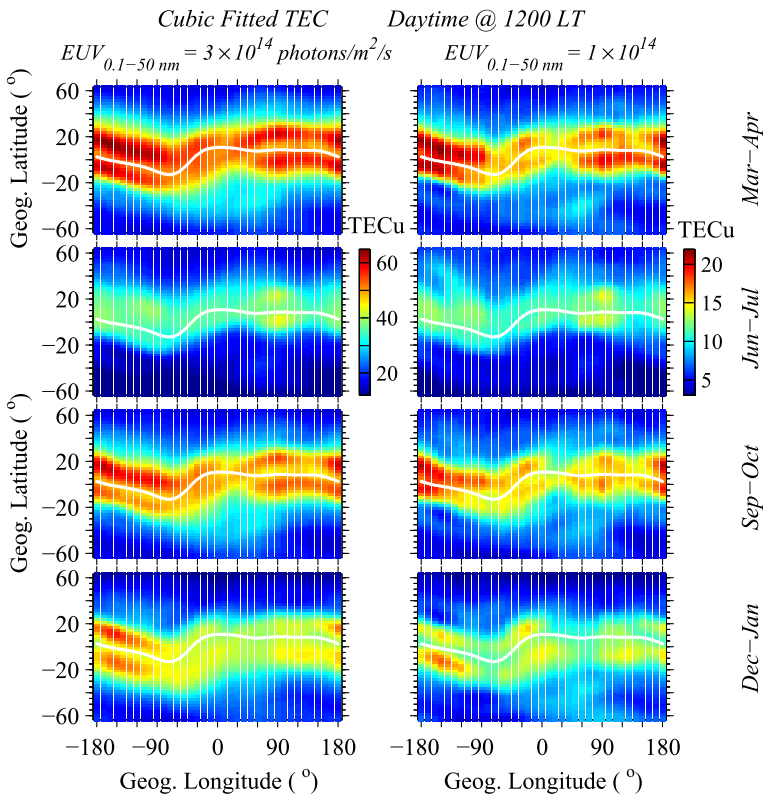

Figure 5 The cubic fitted daytime TEC at two solar EUV levels. Left for the EUV level of 0.1- to 50-nm EUV flux equal to 3 (in units of 10^{14} photons/m^2/s), and right for the EUV level of 0.1- to 50-nm EUV flux equal to 1.

late afternoon is slower at the middle latitudes where dips are close to ±45° (denoted with the dash-dot lines) than at adjacent latitudes. This potentially indicates that the reversal of neutral winds efficiently uplifts the ionosphere to slow down TEC's attenuation at geomagnetic middle latitudes. The slower attenuation of TEC may result in the higher TEC value during nighttime at the middle latitudes where dips are close to ±45°. Under the normal solar cycle condition, the latitudinal difference of TEC's attenuation since the late afternoon is not as prominent as that under the ELSE condition.

In Figure 8, TEC's seasonal variations at different latitudes were investigated with the cubic fitted TEC for the normal solar cycle condition and with the extrapolated TEC for the ELSE condition. For daytime TEC (the left panels of Figure 8), its seasonal variations at the two solar EUV levels are basically similar. The primary feature is the remarkable semiannual variation at geomagnetic low latitudes (about the ±20° band centered on the dip equator); TEC is higher at equinoxes than at solstices. Additionally, there is an annual variation of daytime TEC around the dip equator; TEC is higher at the December solstice than at the June solstice. For nighttime TEC (the right panels of Figure 8), however, its seasonal variation changes with decreases in solar EUV. Under the normal solar cycle condition, seasonal variation of nighttime TEC is dominated by the semiannual variation (higher TEC at equinoxes than at solstices) at the dip equator, whereas the annual variation (higher TEC during the local summer than in other seasons at middle latitudes) becomes dominant with increases in geomagnetic latitude. Under the ELSE condition, this latitudinal difference of TEC's seasonal variation declines. The prominent semiannual variation not only exists at the dip equator but also extends to higher geomagnetic latitudes, as shown by the two TEC peak bands in the right-bottom panel of Figure 8.

Seasonal variation of nighttime TEC also could be affected by neutral winds at geomagnetic middle latitudes. Under normal solar cycle conditions, TEC's annual variation (higher TEC during the local summer than in other seasons) is dominant at middle latitudes during the nighttime, possibly owing to the fact that solar EUV irradiance lasts longer during the local summer than in other seasons and thus can compensate recombination loss to slow down TEC's attenuation to some extent. As the top panels of Figure 7 show, in the late afternoon and around sunset, TEC's attenuation is slower during the local summer than in the two equinoxes at middle latitudes, especially in the northern hemisphere. Whereas with decreasing solar EUV, the increasing neutral winds (Kawamura et al.

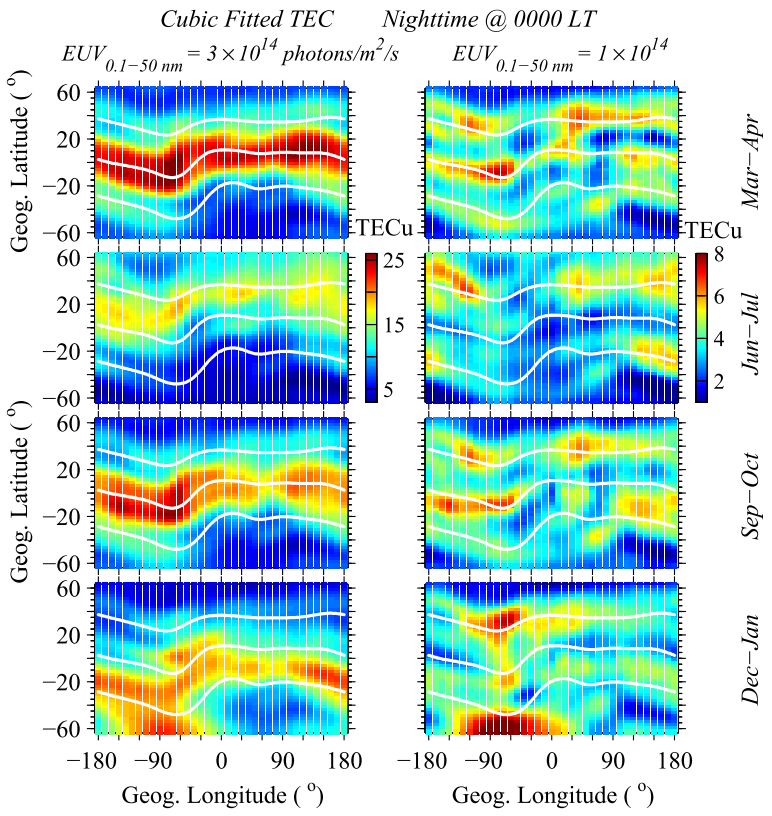

Figure 6 Same as Figure 5 but for nighttime TEC. Three lines in each panel denote the dip equator and dip = ±45° latitudes, respectively.

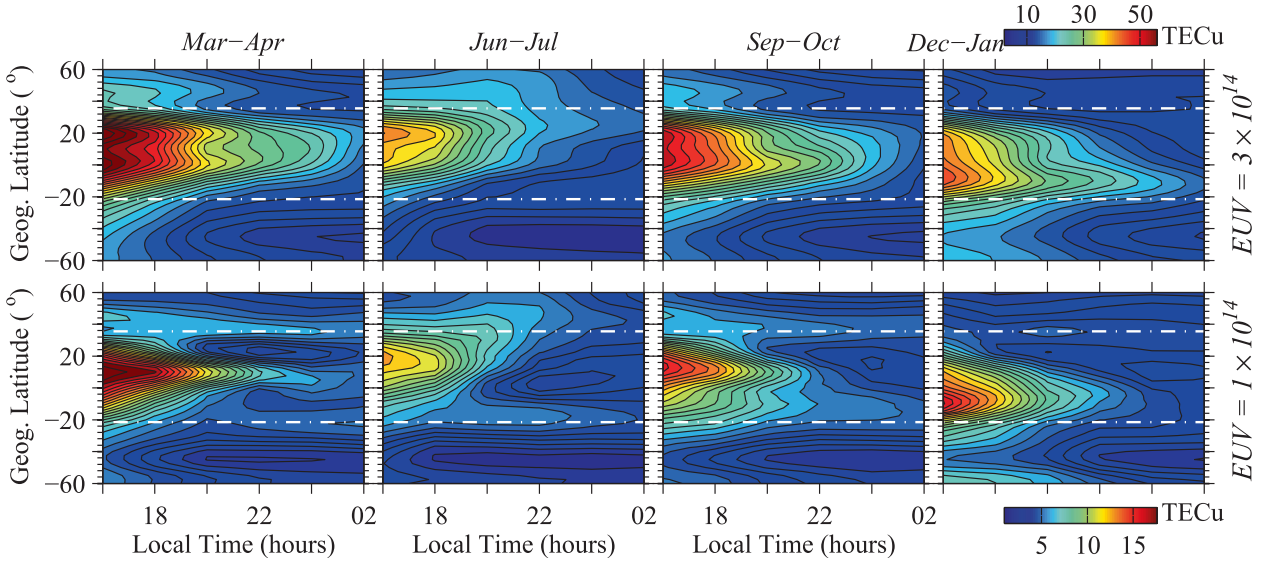

Figure 7 Local time variations of the cubic fitted TEC at 120°E. Top for normal solar cycle condition, and bottom for ELSE condition. The dash-dot lines correspond to dip = ±45° latitudes.

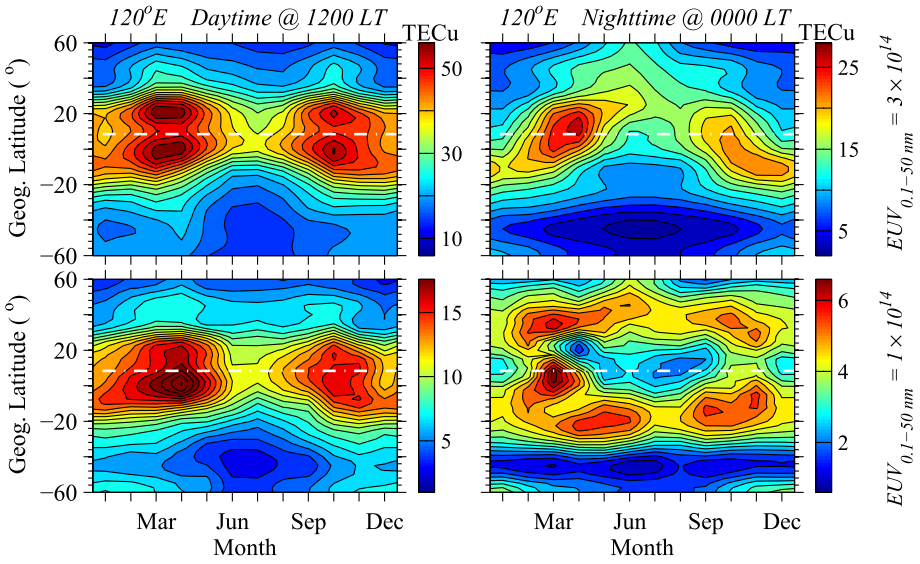

Figure 8 Seasonal variations of the cubic fitted TEC at 120°E. Top for normal solar cycle condition, and bottom for ELSE condition. Left for daytime TEC, and right for nighttime TEC. The dash-dot line denotes the dip equator.

2000; Liu et al. 2004) are possibly strong enough to significantly uplift the ionosphere during the nighttime to slow down TEC's attenuation at the middle latitudes, where dips are close to ±45°, in all seasons, just as the bottom panels of Figure 7 illustrate. In that case, seasonal variation of nighttime TEC is possibly different from that during normal solar cycles at the mid-latitude bands where dips are close to ±45°.

Ionospheric dynamic processes in different regions may affect the variations of the local ionosphere with EUV

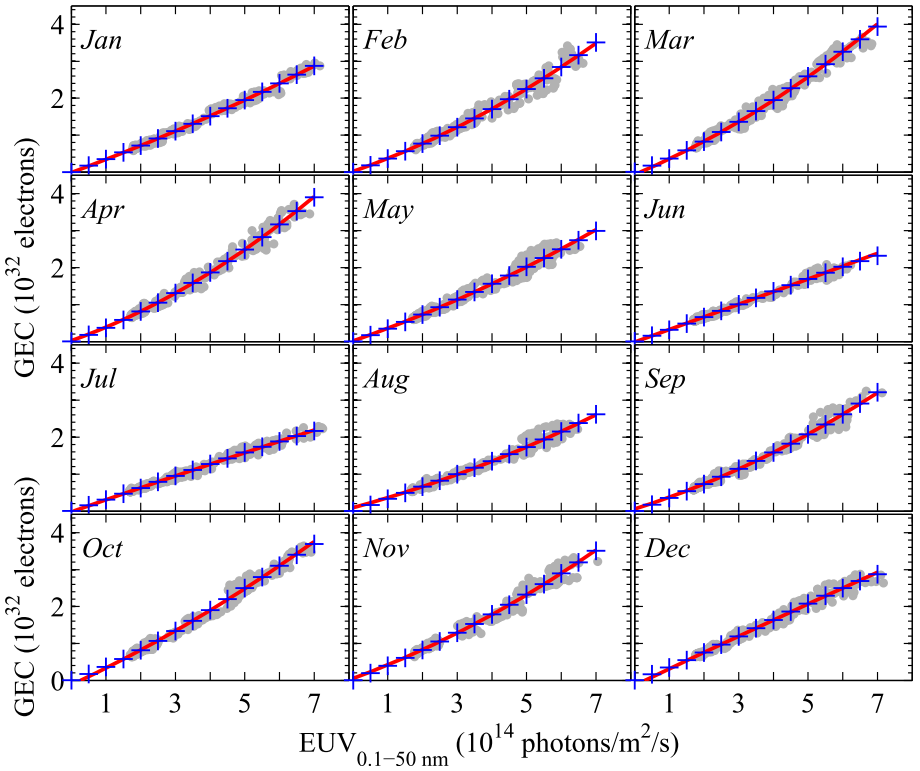

Figure 9 Variations of daily mean GEC with 0.1- to 50-nm EUV flux observed by SOHO/SEM. The solid line is the quadratic fitting of the data, and the cross is the cubic fitting constrained with the term of zero GEC at zero EUV.

(e.g., Chen and Liu 2010; Whalen 2004). If treating the global ionosphere as a whole, how does it vary when solar EUV continuously decreases to ELSE levels? The parameter global electron content (GEC) has been suggested to be a good indicator for detecting solar EUV effects on the global ionosphere (e.g., Astafyeva et al. 2008; Hocke 2008; Liu et al. 2009) because it can suppress some local effects of the ionosphere caused by factors other than solar EUV variability. In this study, we used daily mean GEC to investigate how the global ionosphere varies with decreases in EUV. GEC data were derived from the JPL TEC maps according to Afraimovich et al. (2008).

Figure 9 shows the variations of daily mean GEC with EUV in different months. Quadratic fitting was used to present the dependence of GEC on EUV during the normal solar cycle period. The data indicate that the nonlinearity of GEC-EUV variation is not prominent; GEC nearly increases linearly with EUV in most months. The cubic fitting constrained with the term of zero GEC at zero EUV was used to estimate to what extent the quadratic fitting can describe the GEC-EUV variation under ELSE conditions. The cubic fitting generally agrees with the quadratic fitting very well over most of the EUV range for ELSE conditions. This indicates that the GEC-EUV variation under ELSE conditions should basically follow the GEC-EUV variation trend during the normal solar cycle period.

The dependence of GEC's seasonal variation on solar EUV level was investigated. Figure 10 shows the GEC's seasonal variations at four solar EUV levels. GEC has a prominent semiannual variation during the normal solar cycle period; GEC peaks at the two equinoxes. The annual variation of GEC is also significant; GEC is higher at the December solstice than at the June solstice. With solar EUV decreasing, GEC's seasonal fluctuation declines so that it is relatively small under ELSE conditions, but its primary feature is similar to that during the normal solar cycle period. The increase rate of GEC with EUV, which is listed in Table 1, was approximately derived from the linear GEC-EUV fitting. The GEC-EUV increase rate shows consistent seasonal variation with that of GEC; the increase rate peaks at the two equinoxes and is higher at the December solstice than at the June solstice. The attenuation of GEC's seasonal fluctuation with decreases in solar EUV may be phenomenally explained by this seasonal difference of the dependence of GEC on EUV.

The seasonal variations in the *F* region, where the atomic ion O^+ is dominant, of the global ionosphere are suggested to be closely related to thermospheric parameters such as the thermospheric composition denoted by $[O]/[N_2]$ (e.g., Liu et al. 2007; Mendillo et al. 2005; Rishbeth and Müller-Wodarg 2006). However, the

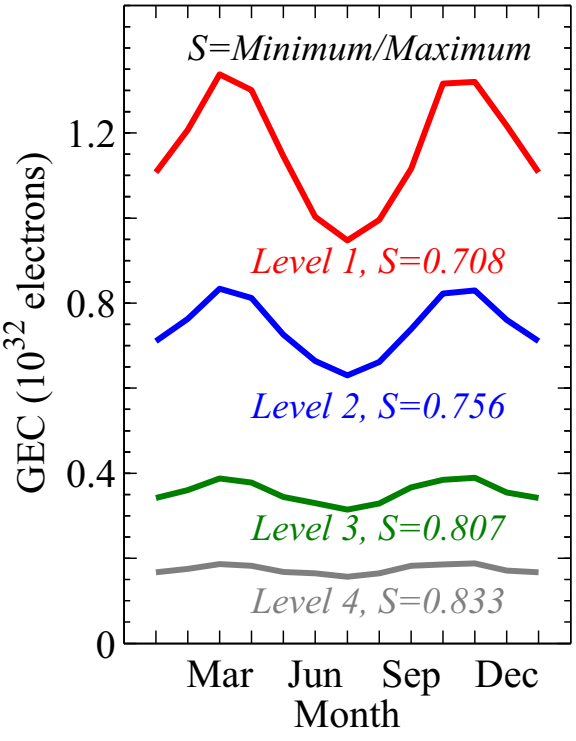

Figure 10 Seasonal variations of the cubic fitted GEC at four solar EUV irradiance levels. Levels 1, 2, 3, and 4 correspond to 0.1- to 50-nm EUV flux equal to 3, 2, 1, and 0.5 (in units of 10^{14} photons/m^2/s), respectively. The parameter *S* equals the ratio of minimum GEC to maximum GEC.

effect of the thermosphere on ionospheric seasonal variations declines with altitude decreasing, because molecular ions gradually become important. The density of molecular ions at lower altitudes is mainly related to EUV flux. For example, the seasonal variation in the *E* region is

Table 1 Global electron content (GEC)-extreme ultraviolet (EUV) increase rate derived from linear GEC-EUV fitting

Month	GEC-EUV increase rate
January	0.422
February	0.513
March	0.602
April	0.580
May	0.435
June	0.342
July	0.314
August	0.365
September	0.462
October	0.565
November	0.510
December	0.436

different from that in the F region. As revealed by Smithtro and Sojka (2005), the ionosphere contracts to lower altitudes with decreases in EUV so that ionospheric electron density peaks at the altitudes where the concentration of molecular ions is equivalent to that of atomic ions, namely, molecular ions become important. Under ELSE conditions, thus, GEC's seasonal fluctuation induced by the variation of thermospheric composition should be less than that under normal solar cycle conditions, owing to the contraction of the ionosphere.

Conclusions

If solar EUV continuously decreases far below the normal solar minimum level, TEC-EUV variation should be nonlinear and may not follow the TEC-EUV variation trend during the normal solar cycle period. We suggest that there are four types of nonlinear TEC-EUV variations over the whole EUV range from zero to the solar maximum level. These nonlinear TEC-EUV variations can be presented with cubic functions of EUV. In terms of the cubic TEC-EUV fitting constrained with the term of zero TEC at zero EUV, we qualitatively discussed the features of the ionosphere under ELSE conditions. The cubic fitting takes not only the available observations but also the extreme ionosphere when solar EUV vanishes into account.

Main climatology features of TEC were investigated with the cubic fitted TEC. Take the solar EUV level of 0.1- to 50-nm EUV flux equal to 1×10^{14} photons/m^2/s, for example, the EIA structure of TEC still exists in daytime, while the latitudinal distribution of TEC is different from that during the normal solar cycle period in nighttime. The seasonal variation of TEC under ELSE conditions is basically consistent with that under normal solar cycle conditions in daytime; however, they are different at middle latitudes in nighttime. Brief discussion indicates that ionospheric dynamic processes still significantly affect the ionosphere under ELSE conditions and may induce some features of TEC different from those under normal solar cycle conditions.

On the global scale, the GEC-EUV variation under ELSE conditions should basically follow the GEC-EUV variation trend under normal solar cycle conditions. GEC has a significant seasonal variation dominated by the semiannual component during the normal solar cycle period; with solar EUV decreasing, GEC's seasonal variation declines so that it is relatively small under ELSE conditions. The contraction of the ionosphere with the solar EUV decreasing possibly results in the attenuation of GEC's seasonal variation.

Competing interests

The authors declare that they have no competing interests.

Authors' contributions

YC performed the statistical analysis and drafted the manuscript. LL, HL, and WW participated in the discussion of the analysis method. All authors read and approved the final manuscript.

Acknowledgements

The SOHO/SEM EUV data were provided by the Space Sciences Center of the University of Southern California. The JPL TEC data were downloaded from the following website: ftp://cddis.gsfc.nasa.gov. This research was supported by Chinese Academy of Sciences (KZZD-EW-01-3), the National Natural Science Foundation of China (41274161, 41231065, 41004068, and 41321003), National Important Basic Research Project of China (2012CB825604 and 2011CB811405), and the National High Technology Research and Development Program of China (2012AA121004).

Received: 21 August 2013 Accepted: 7 March 2014
Published: 12 June 2014

References

Afraimovich EL, Astafyeva EI, Oinats AV, Yasukevich YV, Zhivetiev IV (2008) Global electron content: a new conception to track solar activity. Ann Geophys 26:335–344

Appleton EV (1946) Two anomalies in the ionosphere. Nature 157:691–693

Astafyeva EI, Afraimovich EL, Oinats AV, Yasukevich YV, Zhivetiev IV (2008) Dynamics of global electron content in 1998–2005 derived from global GPS data and IRI modeling. Adv Space Res 42:763–769

Balan N, Bailey GJ, Jenkins B, Rao PB, Moffett RJ (1994) Variations of ionospheric ionization and related solar fluxes during an intense solar cycle. J Geophys Res 99:2243–2253

Chen Y, Liu L, Le H (2008) Solar activity variations of nighttime ionospheric peak electron density. J Geophys Res 113:A11306, doi:10.1029/2008JA013114

Chen Y, Liu L, Wan W, Yue X, Su S-Y (2009) Solar activity dependence of the topside ionosphere at low latitudes. J Geophys Res 114:A08306, doi:10.1029/2008JA013957

Chen Y, Liu L (2010) Further study on the solar activity variation of daytime N_mF_2. J Geophys Res 115:A12337, doi:10.1029/2010JA015847

Chen Y, Liu L, Wan W (2011) Does the $F_{10.7}$ index correctly describe solar EUV flux during the deep solar minimum of 2007-2009? J Geophys Res 116:A04304

Didkovsky LV, Judge DL, Wieman SR (2010) Minima of solar cycles 22/23 and 23/24 as seen in SOHO/CELIAS/SEM absolute solar EUV flux. In: Cranmer SR, Hoeksema JT, Kohl J (eds) SOHO-23: understanding a peculiar solar minimum. Astronomical Society of the Pacific, San Francisco

Eddy JA (1976) The Maunder minimum. Science 192:1189–1202

Emmert JT, Lean JL, Picone JM (2010) Record-low thermospheric density during the 2008 solar minimum. Geophys Res Lett 37:L12102, doi:10.1029/2010GL043671

Fejer BG, de Paula ER, González SA, Woodman RF (1991) Average vertical and zonal F region plasma drifts over Jicamarca. J Geophys Res 96:13901–13906

Fejer BG, Jensen JW, Su S-Y (2008) Quiet time equatorial F region vertical plasma drift model derived from ROCSAT-1 observations. J Geophys Res 113:A05304, doi:10.1029/2007JA012801

Gupta JK, Singh L (2001) Long term ionospheric electron content variations over Delhi. Ann Geophys 18:1635–1644

Hanson WB, Moffett RJ (1966) Ionization transport effects in the equatorial F region. J Geophys Res 71:5559–5572

Hernández-Parajes H, Juan JM, Sanz J, Orus R, Garcia-Rigo A, Feltens J, Komjathy A, Schaer SC, Krankowski A (2009) The IGS VTEC maps: a reliable source of ionospheric information since 1998. J Geod 83:263–275

Hocke K (2008) Oscillations of global mean TEC. J Geophys Res 113:A04302, doi:10.1029/2007JA012798

Iijima BA, Harris IL, Ho CM, Lindqwister UJ, Mannucci AJ, Pi X, Reyes MJ, Sparks LC, Wilson BD (1999) Automated daily process for global ionospheric total electron content maps and satellite ocean altimeter ionospheric calibration based on global positioning system data. J Atmos Sol Terr Phys 61:1205–1218

Judge DL, McMullin DR, Ogawa HS, Hovestadt D, Klecker B, Hilchenbach M, Möbius E, Canfield LR, Vest RE, Watts R, Tarrio C, Kühne M, Wurz P (1998) First solar EUV irradiances obtained from SOHO by the CELIAS/SEM. Sol Phys 177:161–173

Kawamura S, Otsuka Y, Zhang S-R, Fukao S, Oliver WL (2000) A climatology of middle and upper atmosphere radar observations of thermospheric winds. J Geophys Res 105:12777–12788

Lean JL, Woods TN, Eparvier FG, Meier RR, Strickland DJ, Correira JT, Evans JS (2011) Solar extreme ultraviolet irradiance: present, past, and future. J Geophys Res 116:A01102, doi:10.1029/2010JA015901

Liu H, Lühr H, Watanabe S (2007) Climatology of the equatorial thermospheric mass density anomaly. J Geophys Res 112:A05305, doi:10.1029/2006JA012199

Liu L, Luan X, Wan W, Lei J, Ning B (2004) Solar activity variations of equivalent winds derived from global ionosonde data. J Geophys Res 109:A12305, doi:10.1029/2004JA010574

Liu L, Wan W, Ning B, Pirog OM, Kurkin VI (2006) Solar activity variations of the ionospheric peak electron density. J Geophys Res 111:A08304, doi:10.1029/2006JA011598

Liu L, Wan W, Ning B, Zhang M-L (2009) Climatology of the mean total electron content derived from GPS global ionospheric maps. J Geophys Res 114: A06308, doi:10.1029/2009JA014244

Liu L, Chen Y, Le H, Kurkin VI, Polekh NM, Lee C-C (2011) The ionosphere under extremely prolonged low solar activity. J Geophys Res 116:A04320, doi:10.1029/2010JA016296

Mannucci AJ, Wilson BD, Yuan DN, Ho CM, Lindqwister UJ, Runge TF (1998) A global mapping technique for GPS-derived ionospheric total electron content measurements. Radio Sci 33:565–582

Mendillo M, Huang C, Pi X, Rishbeth H, Meier R (2005) The global ionospheric asymmetry in total electron content. J Atmos Sol Terr Phys 67:1377–1387

Richards PG (2001) Seasonal and solar cycle variations of the ionospheric peak electron density: comparison of measurement and models. J Geophys Res 106:12803–12819

Rishbeth H (1972) Thermospheric winds and the F-region: a review. J Atmos Sol Terr Phys 34:1–47

Rishbeth H, Ganguly S, Walker J (1978) Field-aligned and field-perpendicular velocities in the ionospheric F2-layer. J Atmos Terr Phys 40:767–784

Rishbeth H, Müller-Wodarg I (2006) Why is there more ionosphere in January than in July? The annual asymmetry in the F2-layer. Ann Geophys 24:3293–3311

Sethi NK, Goel MK, Mahajan KK (2002) Solar cycle variations of *foF2* from IGY to 1990. Ann Geophys 20:1677–1685

Smithtro CG, Sojka JJ (2005) Behavior of the ionosphere and thermosphere subject to extreme solar cycle conditions. J Geophys Res 110:A08306, doi:10.1029/2004JA010782

Solomon SC, Woods TN, Didkovsky LV, Emmert JT, Qian L (2010) Anomalously low solar extreme-ultraviolet irradiance and thermospheric density during solar minimum. Geophys Res Lett 37:L16103, doi:10.1029/2010GL044468

Strobel DF, Young TR, Meier RR, Coffey TP, Ali AW (1974) The night-time ionosphere: E-region and lower F-region. J Geophys Res 79:3171–3178

Titheridge JE (2000) Modelling the peak of the ionospheric E-layer. J Atmos Sol Terr Phys 62:93–114

Whalen JA (2004) Linear dependence of the postsunset equatorial anomaly electron density on solar flux and its relation to the maximum prereversal E × B drift velocity through its dependence on solar flux. J Geophys Res 109:A07309, doi:10.1029/2004JA010528

doi:10.1186/1880-5981-66-52
Cite this article as: Chen *et al.*: **How does ionospheric TEC vary if solar EUV irradiance continuously decreases?.** *Earth, Planets and Space* 2014 **66**:52.